Large eddy simulation of an ignition front in a heavy duty partially premixed combustion engine

Ibron, Christian; Fatehi, Hesameddin; Jangi, Mehdi; Bai, Xue Song

DOI:
10.4271/2019-24-0010

Large eddy simulation of an ignition front in a heavy duty partially premixed combustion engine

Christian Ibron, Hesameddin Fatehi, Mehdi Jangi, Xue-Song Bai
Lund Institute of Technology, Sweden

ABSTRACT

In partially premixed combustion engines high octane number fuels are injected into the cylinder during the late part of the compression cycle, giving the fuel and oxidizer enough time to mix into a desirable stratified mixture. If ignited by auto-ignition such a gas composition can react in a combustion mode dominated by ignition wave propagation. 3D-CFD modeling of such a combustion mode is challenging as the reaction speed can be dependent on both mixing history and turbulence acting on the reaction wave. This paper presents a large eddy simulation (LES) study of the effects of stratification in scalar concentration (enthalpy and reactant mass fraction) due to large scale turbulence on the propagation of reaction waves in PPC combustion engines. The studied case is a closed cycle simulation of a single cylinder of a Scania D13 engine running PRF81 (81% iso-octane and 19% n-heptane). Two injection timings are investigated; start of injection at -17 CAD aTDC and -30 CAD aTDC. One-equation transported turbulence sub-grid closure is used for the unresolved momentum and scalar fluxes and the fuel spray is modelled using a Lagrangian particle tracking (LPT) approach. Initial flow conditions (prior to intake valve closing) are generated using a scale forcing method with a prescribed large-scale swirl mean flow motion. Fuel reactivity is modeled using finite rate chemistry based on a skeletal chemical kinetic mechanism (44 species, 140 reactions). The results are compared with optical engine experimental data and satisfactory agreement with the experiments is obtained in terms of the liquid spray length, cylinder pressure trace and ignition location. A majority of the fuel consumption is found to be in ignition fronts where small variations in temperature at low fuel concentrations are observed to cause large stratification in ignition delay time.

INTRODUCTION

New internal combustion engine concepts are being developed across the globe to meet the rising demands on efficiency and the increasing restrictions in pollutant emission levels. Among these new concepts it is a common strategy to combust the fuel/air mixture in a low temperature condition to achieve low nitrous oxide ($\mathrm{NO_x}$) emissions while retaining the efficiency benefits of compression ignition engines. This family of low temperature combustion (LTC) engine concepts include members such as partially premixed combustion (PPC) [1, 2], reactivity controlled compression ignition (RCCI) [3], homogeneous charge compression ignition (HCCI) [4] and others. While these concepts are still being developed they often rely on compression ignition in stratified premixed fuel/oxidizer mixtures. Depending on the level of stratification the fuel oxidation can occur in varying modes of combustion, sometimes showing ignition front propagation, non-premixed flame and a premixed flame in the same cycle [5]. Understanding ignition phenomena has long been of interest to the engine community, both in spark ignition engines for the purpose of knock prediction and in diesel engine for the establishment of lift-off lengths. A theory for the propagation of ignition/detonation fronts was laid forth by Zel'dovich [6] who argued that sufficiently small gradients in ignition delay time could cause a reaction front to propagate with a speed inversely proportional to the gradient of ignition delay time. Ergo, to accurately model an ignition front in an engine simulation requires complete information on the stratification of temperature and fuel concentrations at all times during combustion (and to a smaller extent the pressure stratification). This has been investigated for HCCI combustion in constant volume domains with inhomogeneous temperatures in direct numerical simulations [7–9] and others who found that indeed ignition wave and premixed flame front propagation could

co-exist in HCCI combustion, and the mode of combustion is closely correlated with the temperature gradient. In combustion engines the in-cylinder volume decreases as the piston approaches to top dead center (TDC) in the compression cycle, which causes the pressure and temperature to increase, and this gives rise to a non-linear interaction with chemical reactions and heat release. This compression effect was investigated by Bhagatawala et al. [10] who utilized source terms to emulate this decreasing volume effect in direct numerical simulations and found that the effect of emulated pressures influenced the combustion phasing substantially. While small scale turbulent fluctuations exist and affect ignition fronts in engines it is not necessarily the smaller turbulent scales that determine the propagation speed of the front. In a PPC engine or any other direct injection compression ignition engine the gradients in fuel concentration and temperature are caused by multiple effects including fuel injection timing and injection strategies, cylinder gas momentum and temperature distribution.

It is noteworthy that the local temperature difference can vary in the range of 100 K at TDC due to the compression of a gas with small temperature fluctuations [11]. Because of computational limitations the turbulence in engines is often modeled by using large scale filtering (in large eddy simulations, LES) or Reynolds averaging (in Reynolds averaged Navier-Stokes simulations, RANS). This reduces or removes the information of small scale fluctuations. If utilizing a direct integration of reaction rates from finite rate chemistry using a well-stirred reactor (WSR) model, the effect of unresolved scales is ignored and it can result in too low stratification of ignition delay times and thus too fast ignition fronts. This was observed by Ibron et al. in the study of PPC engines with late injection (high stratification) while the same could not be seen for early injections (low stratification) [12]. This work aims to investigate how well the stratification of ignition delay times is represented in a PPC engine using the LES turbulence model that can capture the stratification of fuel and temperature on the scales allowed by the grid. The result is evaluated by comparing heat release rate and cylinder pressure rise rate of the simulation to experimental data. The liquid spray length, pressure trace and ignition location of experimental data will be used to validate the model.

METHODOLOGY AND SETUP

SETUP AND INITIAL CONDITIONS The simulations begin at the start of injection (SOI) for each case but the flow conditions at SOI are calculated in a separate set of simulations unique to each case. Initially the turbulent flow field for pressure, velocity and subgrid turbulence at IVC are obtained from an adiabatic full cylinder LES at intake valve closing (IVC) without piston motion (i.e. constant volume). This simulation begins with with a single large scale motion corresponding to a swirl ratio of 2.2. As this pre-simulation progresses and the large scale kinetic energy breaks into turbulence the large scale motion is superimposed onto the flow so as to keep the swirl ratio

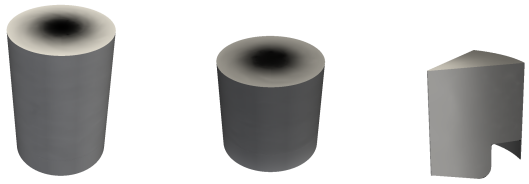

(a) (b) (c)

Figure 1: The steps of acquiring the initial flow field at SOI. From left to right: a) domain for the constant-volume simulation at IVC in which the large scales are modeled using LES to acquire a realistic turbulent flow field; b) domain for the compression cycle LES from IVC to SOI. This non-reacting compression cycle LES is run to obtain the proper thermodynamic initial conditions which are used in the spray injection and combustion cycle LES; c) high resolution periodic sector domain for the spray injection and combustion LES.

constant. This type of large scale forcing continues until the rms of the velocity fluctuations no longer change significantly and the turbulent spectrum is assumed to be stabilized. In order to keep the time at which 50% of the fuel is consumed (CA50) constant in the main simulation the temperature and pressure fields are adjusted for each case after this step. The temperature field is offset with a certain difference and the pressure is scaled with a certain factor unique to each case. After the adjustment in thermodynamic state of the mixture the flow is compressed in a full cylinder LES with regular piston motion and thermodynamic modelling until the SOI of the corresponding case. The fields are then mapped to a high resolution sector mesh for detailed modeling of fuel injection and combustion.

ENGINE CONDITIONS The simulations are performed in a geometry based on an optical Scania D13 heavy duty cylinder with a quartz piston. Geometric simplifications are included in the form of a flat cylinder head with no valve pockets. The simulations are based around the engine conditions visible in Table 1. Because the CA50 combustion phasing mark is kept constant in all simulations the thermodynamic state of the engine gases at IVC differentiated which means that the total mass of air in the simulation varied slightly. This in turn affects the global equivalence ratio for each case accordingly.

NUMERICAL SETUP Because the focus is put on the injection and combustion events which happens close to top dead center (TDC) a periodic 45° sector of the full cylinder is simulated. Separate meshes are used for injection and main combustion in both cases with cell sizes are around 0.22 mm in spray region during injection and 0.45 mm otherwise. Second order linear Gauss schemes are used for spatial discretization and second order backward is used for temporal discretization. The LES turbulence

Table 1: Details of the Scania D13 optical engine experiments in [13], and specification of the conditions used in the LES.

Detail	Value
Bore	130 mm
Squish	1.2 mm
Connecting rod	255 mm
Compression ratio	14.1
Engine speed	1200 rpm
IVC	-160 CAD ATDC
Swirl number	2.2
Domain sector angle	45 deg
Oxygen level (vol.)	21 %
Fuel	PRF 81
Fuel mass (single nozzle)	5.56 mg
Global eq. ratio λ	3.55 - 3.6

model resolves the large scale structures carrying a majority of the kinetic energy. This allows the study of turbulent mixing which is critical to modeling partially premixed combustion. The transport equations are stated below

$$\frac{\partial \bar{\rho}}{\partial t} + \frac{\partial \bar{\rho}\tilde{u}_i}{\partial x_i} = \dot{\rho}^s \tag{1}$$

$$\frac{\partial \bar{\rho}\tilde{u}_i}{\partial t} + \frac{\partial}{\partial x_j}\left(\bar{\rho}\tilde{u}_i\tilde{u}_j - \tilde{\tau}_{ij} - \tau_{ij}^{sgs}\right) = -\frac{\partial \bar{p}}{\partial x_i} + F_i^s \tag{2}$$

$$\frac{\partial \bar{\rho}\tilde{h}}{\partial t} + \frac{\partial}{\partial x_j}\left(\bar{\rho}\tilde{u}_j\tilde{h} - \frac{\bar{\rho}\nu}{Pr}\frac{\partial \tilde{h}}{\partial x_j} - \frac{\bar{\rho}\nu_{sgs}}{Pr}\frac{\partial \tilde{h}}{\partial x_j}\right) = \frac{D\bar{p}}{Dt} + \sum_l \bar{\dot{\omega}}_l h_l + S^s \tag{3}$$

$$\frac{\partial \bar{\rho}\tilde{Y}_l}{\partial t} + \frac{\partial}{\partial x_j}\left(\bar{\rho}\tilde{u}_j\tilde{Y}_l - \bar{\rho}D\frac{\partial \tilde{Y}_l}{\partial x_j} - \bar{\rho}D_{sgs}\frac{\partial \tilde{Y}_l}{\partial x_j}\right) = \dot{\rho}_l^s + \bar{\dot{\omega}}_l \tag{4}$$

where $\dot{\rho}^s$, $\dot{\rho}_l^s$, S^s, F_i^s and $\bar{\dot{\omega}}_l$ are the source terms for mass, momentum and energy equations due to the gas/liquid Lagrangian particle tracking (LPT) coupling and chemical reactions. A straight bar over a variable means the variable are volume filtered while a tilde means Favre filtering. The unresolved transport terms present in the momentum, enthalpy and species equations are closed using a transported one equation subgrid turbulence model that computes the subgrid scale terms using the resolved scale quantities through an eddy viscosity ν_{sgs}, calculated as

$$\nu_{sgs} = C_k\sqrt{k_{sgs}}\Delta \tag{5}$$

where $\Delta = (dxdydz)^{1/3}$ is the characteristic length scale of the cell. The Prandtl number Pr is a known quantity for the gas mixture and a unity Lewis number assumption is used to calculate the species diffusion coefficients D and D_{sgs} from the corresponding viscosity. The unresolved kinetic energy k_{sgs} is modeled using a transport eqaution,

$$\bar{\rho}\frac{Dk_{sgs}}{Dt} - \frac{\partial}{\partial x_j}\left(\bar{\rho}\left(\nu + \nu_{sgs}\right)\frac{\partial k_{sgs}}{\partial x_j}\right) = \bar{\rho}\tau_{ij}^{sgs}\tilde{S}_{ij} - \frac{C_\epsilon k_{sgs}^{3/2}}{\Delta} \tag{6}$$

The coefficients C_k and C_ϵ are constant values set to 0.094 and 1.048 respectively [14]. The subgrid stress tensor is modeled as

$$\tau_{ij}^{sgs} = 2\bar{\rho}\nu_{sgs}\tilde{S}_{ij} - \frac{2}{3}\bar{\rho}k_{sgs}\delta_{ij} \tag{7}$$

and this closes the model for the resolved scale momentum transport. For scalar transport fluxes similar models are used.

The fuel injection is modeled using Lagrangian particle tracking (LPT) method that represents the statistical distribution of fuel droplets by tracking so-called parcels. The parcels interact with the gas flow in a two-way coupling. The primary breakup and atomization of the droplets are modeled using the Kelvin-Helmholtz/Rayleigh-Taylor (KHRT) breakup model with standard coefficients [15], except for the breakup timescale coefficient B_1, which is set to 20. The injected size of the parcels is chosen randomly from a Weibull distribution with a k value of 3 and an average diameter of 60 μm. The parcels react with a partially plastic rebound on wall collisions.

Chemistry is modeled using a finite rate chemical kinetic mechanism for calculation of instantaneous reaction rates. These are calculated using the Arrhenius formula with coefficients from a reduced reaction mechanism for PRF fuel using 44 species and 144 reactions [16]. The reaction rates are obtained through direct integration for each time step. This means that the effect of the unresolved stratification will not be modeled.

The chemical reaction rates are integrated into the transport equations using chemistry coordinate mapping, an efficient speedup algorithm [17], in which the calculation of reaction rates are not performed for individual mesh cells but for groups of cells, where the grouping is determined in a so-called chemistry phase space. This phase space is made up of six dimensions in this study: a progress variable based on element mass fractions, scalar dissipation rate, temperature, and mass fractions of fuels and nitrogen gas. This speedup method has been validated for the SOI-17 case and showed deviations on the level of numerical errors only.

ANALYSIS METHODS A probability density function (PDF) is defined to quantify the stratification of a general scalar ϕ:

$$p(\phi = \psi)_{fuel} = \sum_{cell}\frac{V\cdot\rho\cdot Z\cdot\delta(\phi-\psi)}{V\cdot\rho\cdot Z} \tag{8}$$

where Z_j is the mixture fraction of gas in the j-cell, V_j is the volume of the j-cell, ρ_j is the gas density in the j-cell and δ is the Kronecker delta-function. In this definition PDF of a scalar ϕ is weighted by the mass originated from the fuel injected into the cylinder.

One of the methods to prove the presence of ignition fronts in domain is comparing the reaction rate source

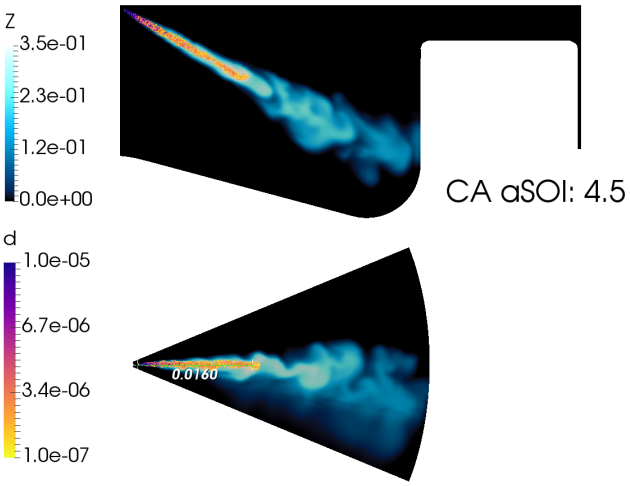

Figure 2: Cross-sectional view of instantaneous spray plume showing the mixture fraction (Z) and parcel Sauter mean diamater size distribution (d) during quasi-steady state injection stage in the LES-17 case. The plane normals are perpendicular to each other and both planes cut the center of the spray.

term to the diffusive term in the transport equation of some species, cf. equation 4. The combustion mode is said to be ignition front dominant if the magnitude of the reaction rate term is an order of magnitude higher than the diffusive transport term, whereas otherwise it is a flame front. This method is commonly found in DNS work where the diffusive term in a species transport is fully resolved. In the simulations presented below the effect of the unresolved subgrid scalar flux is included in the diffusive term through the subgrid scale model. The method is used here to prove the presence of an ignition front.

RESULTS AND DISCUSSION

VALIDATION

Spray Figures 2 and 3 show the quasi-steady liquid penetration lengths for both simulated cases. The penetration length (95% liquid mass) value is calculated by projecting the actual liquid length onto the plane perpendicular to the piston axis. This allows a qualitative comparison to the liquid length observed in the Mie scattering images observed by Lönn et al., cf. Fig. 4. The experimentally observed quasi-steady liquid length for the SOI-17 case is 15-16 mm, which correlates well with the simulation value of 16 mm. The experimentally observed liquid penetration for the LES-30 case is 25 mm, which correlates also very well with the value of 26 mm from the simulation.

Ignition location The ignition location is observed in the experiments by means of natural luminosity which has no direct equivalent to the simulated flow and scalar variables. It can be argued that both temperature and heat release rate correlate with the natural luminosity and both

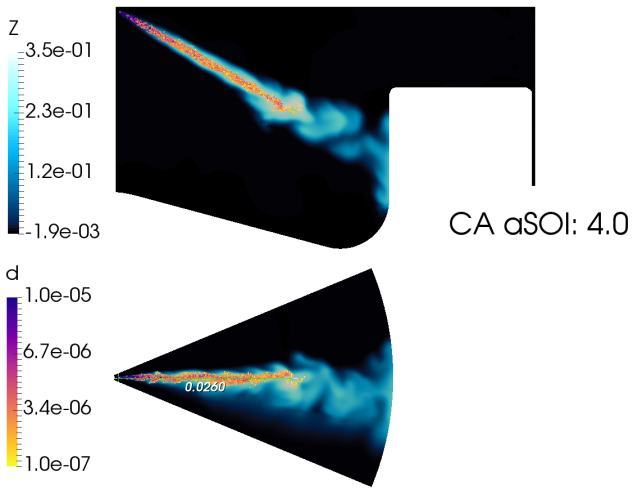

Figure 3: Cross-sectional view of instantaneous spray plume showing the mixture fraction (Z) and parcel Sauter mean diamater size distribution (d) during quasi-steady state injection stage in the LES-30 case. The plane normals are perpendicular to each other and both planes cut the center of the spray.

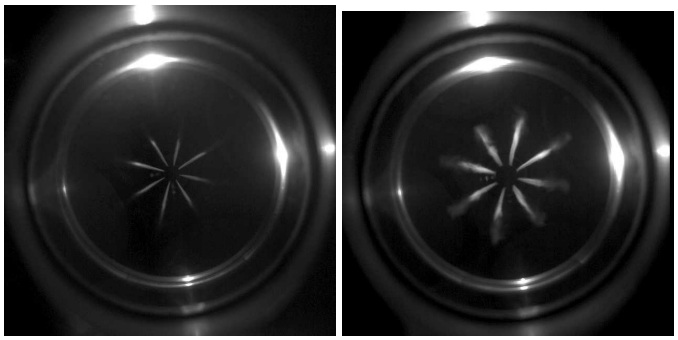

Figure 4: Mie scattering of SOI-17 and SOI-30 in quasi steady spray [13]

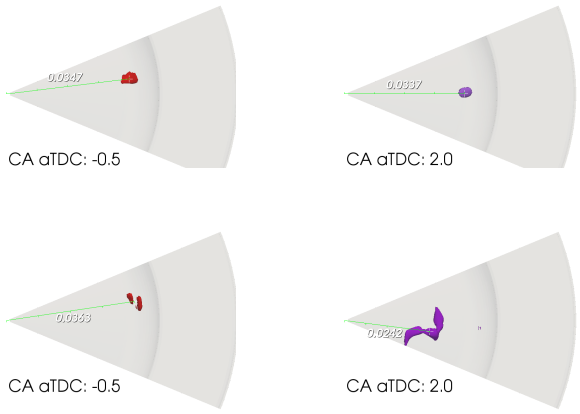

Figure 5: Ignition locations for cases SOI-17 (top row) and SOI-30 (bottom row). The heat release rate criterion of $5 \cdot 10^9 \mathrm{J} \cdot \mathrm{s}^{-1} \cdot \mathrm{m}^{-3}$ is used for identifying ignition kernels in the left row while the ignition kernel in the right column is identified by means of iso-temperature of 1300 K.

criteria are used for determining the radial ignition location of the ignition sites, cf. Fig. 5. Both methods for ignition location are well within the experimentally observed standard deviation as seen in Fig. 6.

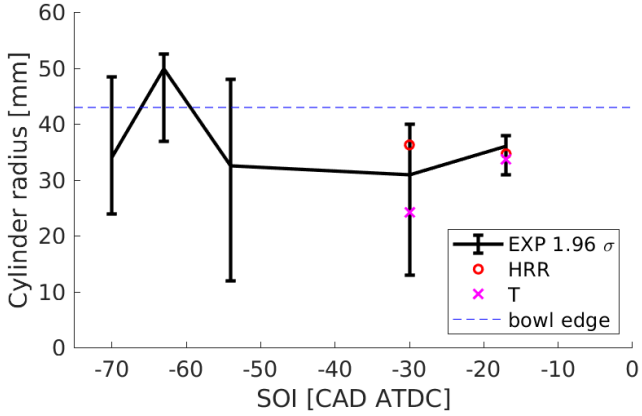

Figure 6: The black line shows experimentally observed radial ignition location as a function of the injection timing with corresponding bars showing the range of cycle-to-cycle variation of the ignition location. Ignition locations based on criteria of heat release rate (HRR) and temperature (T) are shown in red circles and purple cross symbols.

Cylinder average pressure Figures 7 and 8 show the comparison of cylinder pressure from the experiment and simulations for the SOI-17 and SOI-30 cases, respectively. The LES replicates very well the pressure traces. It is shown that the SOI-17 has a higher pressure rise rate after TDC than the SOI-30 case, whereas the SOI-30 case has a higher cycle-to-cycle variation. The SOI-17

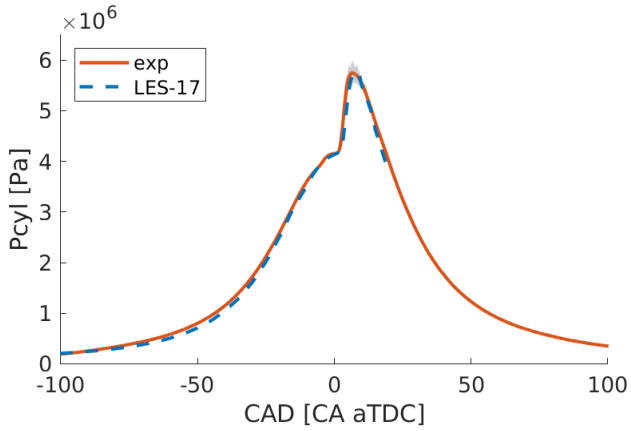

Figure 7: A comparison of the cycle average cylinder pressure in the experiment and the simulation for case SOI-17. The single cycle pressure traces from the experiments are shown in the background in grey color. The simulated pressure is well within the cycle-to-cycle variations of the experiments.

case has a later fuel injection and thus a higher levels of temperature and composition stratification than the case of SOI-30. The CA50 in both cases are maintained by increasing the initial temperature of the SOI-17 case, which partially contributes to the higher heat release rate and thus a higher pressure-rise rate in the SOI-17 case. To gain deeper insight into the combustion and heat release process it is necessary to examine the detailed scalar fields obtained in LES, in particular, the temporal evolution and spatial distribution of these quantities.

Reaction front identification Figure 9 shows a comparison of the diffusion transport term and reaction rate term of the mass fraction of CO_2 for all computational cells in the domain during the combustion process in both cases. Because the reaction rate term in most cells is several orders of magnitude larger than the diffusive transport term, or at least one order of magnitude larger than the highest diffusive term, the proof that ignition front propagation dominates the combustion process can be considered strong. The graph shows that there are cells that the diffusion terms are of comparable magnitudes as the reaction rate terms, which indicates the possibility of having a premixed flame propagation, but this is rather rare at the shown 4 CAD aTDC.

To examine the spatial distribution of the reactive scalars and their temporal evolution, Figure 10 shows spatial distribution of CO mass fraction and an iso-contour of OH mass fraction in a cross section middle of the sector domain. OH radicals are indicator of the second-stage (high temperature) ignition of the PRF fuel. As seen at 2.5 CAD aTDC the OH contour encloses only a small region of the domain in both cases, indicating that the process is in the

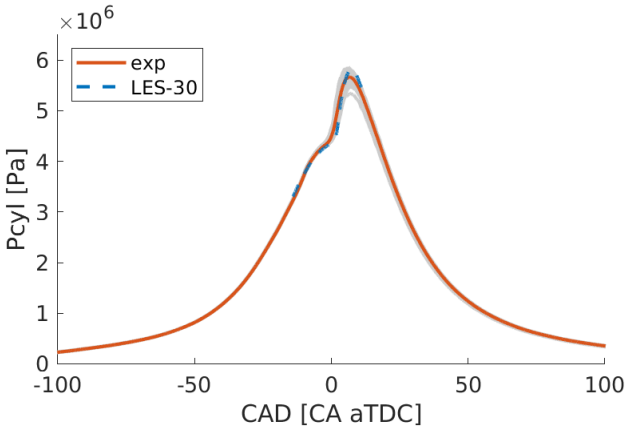

Figure 8: A comparison of the cycle average cylinder pressure in the experiment and both simulations for case SOI-30. The single cycle pressure traces from the experiments are shown in the background in grey color. The simulated pressure is well within the cycle-to-cycle variations of the experiments.

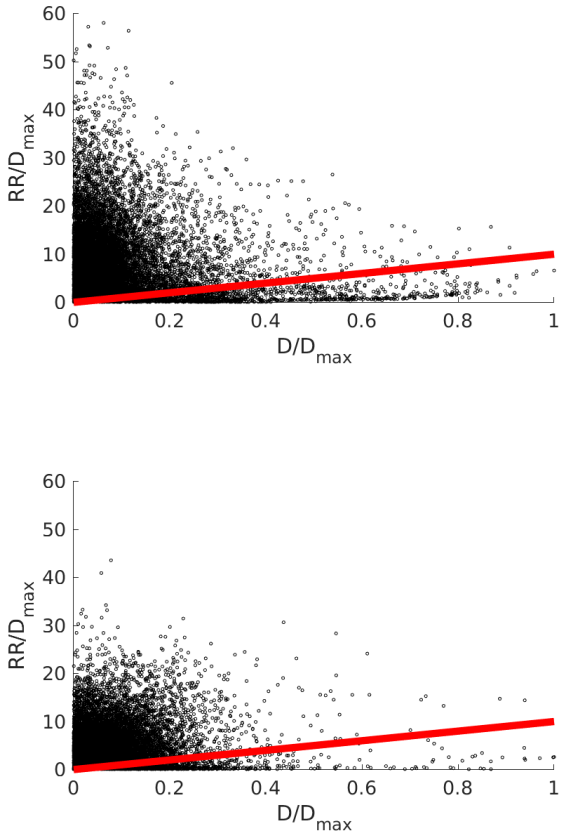

Figure 9: A scatter plot of chemical reaction rate and diffusive transport term in the transport equation of the mass fraction of CO_2 in each cell for case SOI-17 (upper row) and case SOI-30 (lower row) at 4 CA aTDC (around CA50). The values of reaction rate terms and diffusion terms are normalized by the maximum diffusive term value in each case. The red line depicts the limit where the local reaction rate is an order of magnitude greater than the diffusion term.

earlier ignition stage. At this stage CO is shown to distribution in large region of the domain. It appears that CO is already formed during the first-stage (low temperature) ignition, before the onset of second-stage ignition. The fuel is converted to CO in the first-stage ignition, and CO is converted to CO_2 in the second stage ignition by reaction of CO + OH = CO_2 + H_2. Since this reaction is very fast CO and OH are hard seen to co-exist in the domain, cf. Fig. 10. By comparing the CO field and the OH iso-contour it is evident that the reaction front of CO and OH propagate through a large region of domain within just 2.5 CAD, which is only possible by virtue of ignition wave propagation.

STRATIFICATION ANALYSIS The pressure rise rate of the experimental pressure traces and the combustion duration shown in the natural luminosity images in Ref. [13] show that the ignition event in the SOI-17 case is substantially faster than in the SOI-30 case. Both cases are dominated by ignition front combustion initially as shown above, which implicates that the spread of ignition delay time in the SOI-17 case is lower than for the SOI-30 case. This can be considered counter-intuitive since the later injection timing means the stratification in both temperature and mixture fraction is higher. The stratification in the composition and temperature has been observed in the simulations and is depicted in Fig. 11, which shows probability density functions of temperature and mixture fraction prior to the ignition (-5 CA aTDC). Because of the early injection in the SOI-30 case the fuel has had more time to dwell in a low temperature environment. To maintain the same CA50 for the SOI-17 case as that in the SOI-30 case, the initial temperature in the SOI-30 case has to be lower than that in the SOI-17 case (in the experiments and also proven in the simulations). Due to the negative temperature coefficient (NTC) effect in PRF fuels the low temperature ignition reactions and the high temperature reactions are different in the two cases. The NTC effect results in a ”cool flame” which releases heat prior to the main ignition, heating up the mixtures. This can be seen in the temperature PDF of the SOI-30 case in Fig. 11, where a majority of the fuel can be found in the range between 950 K and 1000 K. This cool flame effect is present but weaker for the SOI-17 case as the fuel has less time to dwell in a low temperature environment. The combined effects of late injection and less cool flames causes the temperature stratification to be much higher for the SOI-17 case. The stratification in terms of fuel concentration is larger for the later injection timing as would be expected. The reason why the effective spread in ignition delay times is broader in the SOI-30 case is because of the non-linear dependence of ignition delay time on temperature and fuel concentration. More specif-

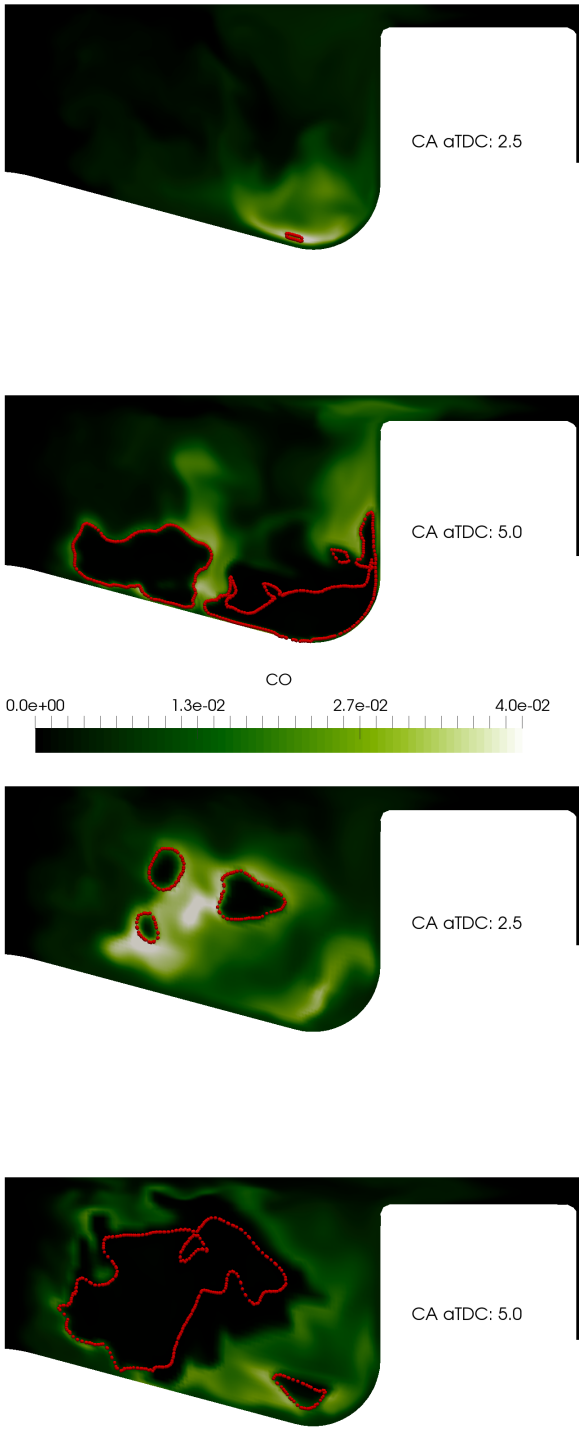

Figure 10: The mass fractions of CO for the SOI-17 case (top row) and SOI-30 case (bottom row) at the onset of high temperature ignition (2.5 CAD aTDC) and during the movement of the ignition front (5 CAD aTDC). The shown plane is cutting through the middle of the sector. An isoline of OH mass fraction shows the high temperature ignition front that encloses the burned gas (the low CO region).

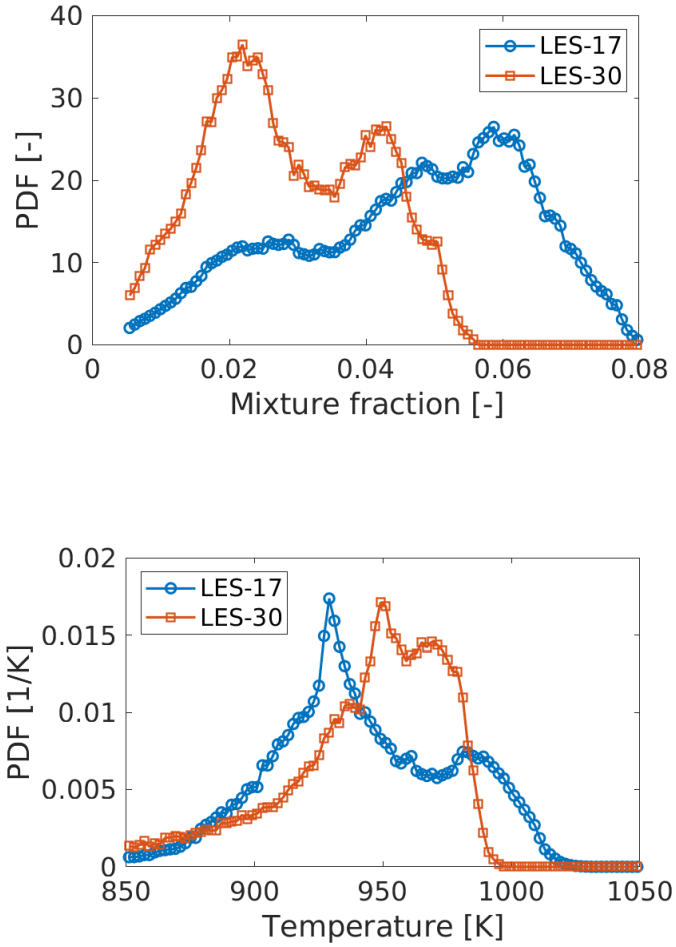

Figure 11: The probability density functions of mixture fraction (top) and temperature (bottom) at -5 CA aTDC for the SOI-17 and SOI-30 cases. The probability calculation is weighted by the fuel mass of each cell so the PDFs show the probability of the fuel only, not the gas composition as a whole. The late injection case shows stronger stratification in terms of both temperature and mixture fraction

ically for iso-octane at lower mixture fractions, the ignition delay time dependence on temperature is much more higher than it is close to stoichiometry [18, 19]. For the present PRF81 fuel numerical simulation of ignition process in homogeneous mixtures under conditions relevant to the present PPC engines show that

$$\begin{aligned} \left|\frac{\partial \tau}{\partial T}|_{Z=0.03}\right| &> \left|\frac{\partial \tau}{\partial T}|_{Z=0.06}\right|, \\ \left|\frac{\partial \tau}{\partial Z}|_{Z=0.03}\right| &> \left|\frac{\partial \tau}{\partial Z}|_{Z=0.06}\right|, \end{aligned} \tag{9}$$

This causes the stratification of the ignition delay time to be larger in the early injection case (SOI-30) which in turn causes a slower ignition front propagation.

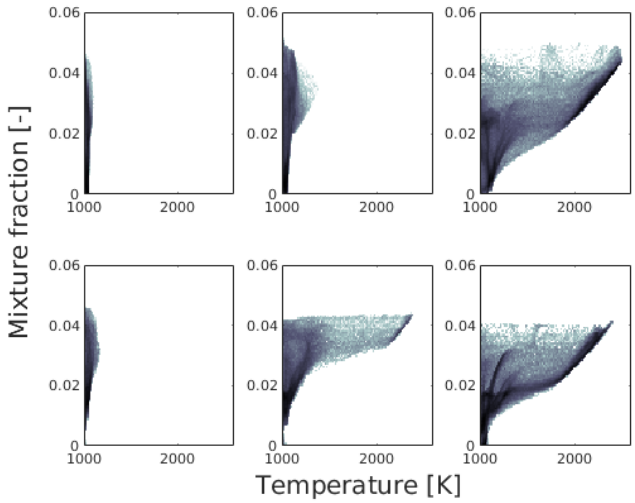

Figure 12: The progression of the joint probability density function conditioned on temperature and mixture fraction of the cylinder gas in the SOI-17 case (top row) and SOI-30 case (bottom row). The columns correspond to times 0, 2 and 5 CA aTDC chronologically set from left to right.

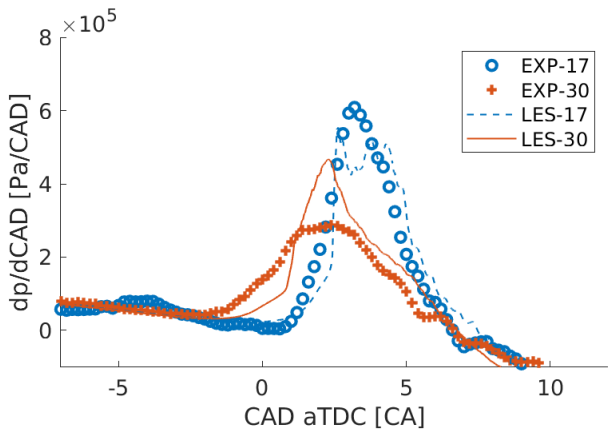

Figure 13: An in-cylinder pressure time-derivative comparison between and simulations and experiments. The experimental pressure derivative are obtained from the cycle averaged pressure and a low temporal resolution (0.2 CA sampling frequency) while the pressure derivative from the simulations are based on the time step of the simulation (in the order of 10^{-7} seconds).

IGNITION AND COMBUSTION ANALYSIS The experimentally observed onset of ignition for the SOI-17 case is between 2-3 CA aTDC [13], which is replicated well in the LES-17 simulation. In the SOI-17 case the fuel from the spray impinges in the bottom part of the bowl as seen in Fig. 2 and the spray stream is rebounded upward to the squish and back into the center of the bowl. As the fuel gas flow is slowed down by the shear forces and mixed with the cylinder air the swirl transports the bulk of the fuel cloud, further mixing it with the surrounding gas. A fraction of the fuel cloud positioned close to the piston remains in a richer state as the swirl is weaker close to the piston wall. This location is the first to reach heat release rates that signify main ignition, cf. Figs. 5 and 10. The initial kernel is quite lean and has a mixture fraction of roughly 0.036. Due to the small cylinder volume near TDC the released heat in the system causes the pressure to rise and through thermodynamic coupling it increases the gas temperature, causing an explosive feedback loop between the gas temperature and the combustion. This is seen in the simulation as the initial ignition kernel which appeared around 2 CA aTDC suddenly expands to consume the majority of the richer fuel region by the time of 5 CA aTDC. This progress is seen in mixture fraction and temperature space in Fig. 12 where most of the richer regions ($0.03 < Z < 0.06$) are seen to be suddenly in a high temperature state at the time 5 CA aTDC while the leaner regions remain unburned. This agrees well with the statement of ignition wave spreading in the previous section - the rich regions have low stratification in ignition delay times despite high temperature stratification while unburned. The presence of an ignition front is less obvious after 7 CA aTDC where the diffusive and reactive terms of CO_2 mass fraction reach similar magnitudes and the displacement of the reactive front slows down to speeds which can occur in turbulent premixed flames.

For the SOI-30 case the fuel vapor impinges on the vertical piston wall as seen in Fig. 3 and follows the shape of the wall down into the bottom of the bowl and the into the center. Spray induced turbulence and shear caused by swirl dilutes the fuel cloud while the NTC effect starts building up. Because of the cooler cylinder gas temperature the NTC effect is stronger than in the SOI-17 case and the cool flame propagates at -10 CA aTDC heating up the fuel. The reactions begin in a large volume in the middle of the cylinder at roughly -2 CA aTDC and slowly spreads into the rest of the volume over a time span of five crank angles. The original ignition kernel is close to the richest point of the mixture with a mixture fraction of 0.035. Because of the stratification in ignition delay time the ignition front propagates much slower than for the SOI-17 case as seen in Fig. 12. Since most of the fuel is in a very lean state (mixture fraction around 0.02) the stratification in ignition delay time is high due to temperature. Figure 12 shows how the leaner parts are starting to react at 5 CA aTDC. While it is again hard to say when deflagration wave overtakes ignition wave some parts of the reaction front in the SOI-30 case slow down to displacement speeds similar to turbulent flames as soon as 3 CA aTDC but this could still be a stratified slow ignition front. In any case the reaction front displacement is more dependent on the effects of the flow, which can be considered ”frozen” during the fast part of the ignition front. This partially invalidates the assumption that unresolved scalars will not affect the filtered reaction rates.

The averaged pressure-rise rate of the experiments is compared to the simulated results in Fig. 13. The figure shows qualitative agreement in both cases but a better match for the SOI-17 case. One reason could be that

the resolved stratification is insufficiently modeled - either due to unresolved stratification or sector assumption. A third possible reason can be that the well stirred reactor assumption is better for the cases where the ignition front is faster. This implies that the unresolved flow affects the ignition front in the SOI-30 case, more on the reaction rate than on the diffusion terms, due to the difference in magnitudes in reaction rates and diffusive terms as seen in Fig. 9.

CONCLUSIONS

Large eddy simulations are carried out to study the combustion process of a PRF fuel in a PPC engine cylinder. The fuel is a mixture of 81% iso-octane and 19% n-heptane (on volume basis). Two injection timings are considered in the study. The combustion phasing, in terms of CA50, is maintained constant in the two cases by adjusting the initial temperature of the mixture before fuel injection. The LES spray combustion model properly replicates the optical experimental observations, in terms of in-cylinder pressure, onset of ignition timing and spatial location, and spray penetration length. The LES data are used to gain deeper insight into the combustion process. The following conclusions could be drawn:

- The dominant mode of combustion in the present PPC cases is ignition front propagation. This is evidenced by the much higher reaction rates as compared with the diffusive transport term of CO_2 mass fraction and the rapid spreading of the high temperature ignition front in the cylinder that converts the CO to CO_2.
- Given that the combustion is dominated by a fast propagation of the ignition front, sufficiently fine resolution of the stratification in the composition and temperature of the mixture appears to be important to obtain good agreement between experiments and simulations in ignition location and combustion phasing.
- In a PPC engine with PRF fuel a later injection can result in a fuel-richer mixture, a smaller stratification in ignition delay time, and a higher pressure-rise rate, despite having larger stratification in temperature and mixture fraction compared with an earlier injection. The reason for this is identified as that the ignition delay time is more sensitive to the variation of temperature and mixture fraction under fuel-lean conditions than under fuel-richer conditions.

ACKNOWLEDGEMENTS

This work was sponsored by the Swedish Research Council and Kompetenscenter för Förbränningsprocesser (the KCFP project) at Lund University. The CFD simulations were performed on resources provided by the Swedish National Infrastructure for Computing (SNIC) at PDC and HPC2N centers.

References

[1] Gautam T. Kalghatgi, Per Risberg, and Hans-Erik Ångström. “Partially Pre-Mixed Auto-Ignition of Gasoline to Attain Low NOx aat High Load in a Compression Ignition Engine and Comparison with a Diesel Fuel”. In: *SAE Technical Paper 2007-01-0006*. 2007.

[2] Vittorio Manente, Claes-Goeran Zander, Bengt Johansson, Per Tunestal, et al. “An Advanced Internal Combustion Engine Concept for Low Emissions and High Efficiency from Idle to Max Load Using Gasoline Partially Premixed Combustion”. In: *SAE Technical Paper 2010-01-2198*. SAE International, Mar. 2010. URL: http://dx.doi.org/10.4271/2010-01-2198.

[3] Kazuhisa Inagaki, Takayuki Fuyuto, Kazuaki Nishikawa, Kiyomi Nakakita, et al. “Dual-Fuel PCI Combustion Controlled by In-Cylinder Stratification of Ignitability”. In: *SAE 2006-01-0028*. Apr. 2006. URL: http://papers.sae.org/2006-01-0028/.

[4] Shuji Kimura, Osamu Aoki, Hiroshi Ogawa, Shigeo Muranaka, et al. “New combustion concept for ultra clean and high efficiency small DI diesel engine.pdf”. In: *SAE Technical Paper 1999-01-3681*. 1999. ISBN: 0148-7191.

[5] Mark P.B. Musculus, Paul C. Miles, and Lyle M. Pickett. “Conceptual models for partially premixed low-temperature diesel combustion”. In: *Progress in Energy and Combustion Science* 39 (Apr. 2013), pp. 246–283. URL: http://linkinghub.elsevier.com/retrieve/pii/S0360128512000548.

[6] Ya.B. Zeldovich. “Regime classification of an exothermic reaction with nonuniform initial conditions”. In: *Combustion and Flame* 39 (Oct. 1980), pp. 211–214. URL: https://www.sciencedirect.com/science/article/pii/0010218080900176.

[7] R. Sankaran and H. G. Im. “Characteristics of autoignition in a stratified iso-octane mixture with exhaust gases under homogeneous charge compression ignition conditions”. In: *Combustion Theory and Modelling* 9.3 (Aug. 2005), pp. 417–432. ISSN: 1364-7830. URL: http://www.tandfonline.com/doi/abs/10.1080/13647830500184108.

[8] Jacqueline H Chen, Evatt R Hawkes, Ramanan Sankaran, Scott D Mason, et al. “Direct numerical simulation of ignition front propagation in a constant volume with temperature inhomogeneities I. Fundamental analysis and diagnostics”. In: *Combustion and Flame* 145 (2006), pp. 128–144. URL: www.elsevier.com/locate/combustflame.

[9] Rixin Yu and Xue-Song Bai. “Direct numerical simulation of lean hydrogen/air auto-ignition in a constant volume enclosure”. In: *Combustion and Flame* 160.9 (Sept. 2013), pp. 1706–1716. ISSN: 0010-2180. URL: https://www.sciencedirect.com/science/article/pii/S0010218013001259.

[10] Ankit Bhagatwala, Ramanan Sankaran, Sage Kokjohn, and Jacqueline H. Chen. “Numerical investigation of spontaneous flame propagation under RCCI conditions”. In: *Combustion and Flame* 162 (Sept. 2015), pp. 3412–3426. URL: https://www.sciencedirect.com/science/article/pii/S0010218015001844.

[11] R. Yu, T. Joelsson, X. S. Bai, and Bengt Johansson. “Effect of Temperature Stratification on the Autoignition of Lean Ethanol/Air Mixture in HCCI engine”. In: June 2008. URL: http://papers.sae.org/2008-01-1669/.

[12] Christian Ibron, Mehdi Jangi, Sara Lonn, Alexios Matamis, et al. “Effect of Injection Timing on the Ignition and Mode of Combustion in a HD PPC Engine Running Low Load”. In: Apr. 2019. URL: https://www.sae.org/content/2019-01-0211/.

[13] Sara Lonn, Alexios Matamis, Martin Tuner, Mattias Richter, et al. “Optical Study of Fuel Spray Penetration and Initial Combustion Location under PPC Conditions”. In: *SAE Technical Paper 2017-01-0752*. Mar. 2017. URL: http://papers.sae.org/2017-01-0752/.

[14] Pierre Sagaut. *Large eddy simulation for incompressible flows : an introduction*. Springer-Verlag, 2006, p. 556.

[15] Rolf D. Reitz and Jennifer C. Beale. “Modeling spray atomization with the Kelvin-Helmholz/Rayleigh-Taylor Hybrid Model”. In: *Atomization and Sprays* 9 (1999), pp. 623–650. URL: http://www.dl.begellhouse.com/journals/6a7c7e10642258cc,2b018a87685a3d87,76af95984924bb68.html.

[16] Yao-Dong Liu, Ming Jia, Mao-Zhao Xie, and Bin Pang. “Enhancement on a Skeletal Kinetic Model for Primary Reference Fuel Oxidation by Using a Semidecoupling Methodology”. In: *Energy & Fuels* 26 (Dec. 2012), pp. 7069–7083. URL: http://pubs.acs.org/doi/10.1021/ef301242b.

[17] Mehdi Jangi and Xue-Song Bai. “Multidimensional chemistry coordinate mapping approach for combustion modelling with finite-rate chemistry”. In: *Combustion Theory and Modelling* 16 (Dec. 2012), pp. 1109–1132. URL: http://www.tandfonline.com/doi/abs/10.1080/13647830.2012.713518.

[18] K. Fieweger, R. Blumenthal, and G. Adomeit. “Self-ignition of S.I. engine model fuels: A shock tube investigation at high pressure”. In: *Combustion and Flame* 109.4 (June 1997), pp. 599–619. ISSN: 0010-2180. URL: https://www.sciencedirect.com/science/article/abs/pii/S0010218097000497.

[19] Janardhan Kodavasal and Sibendu Som. “Gasoline Compression IgnitionA Simulation-Based Perspective”. In: Springer, Singapore, 2018, pp. 227–249. URL: http://link.springer.com/10.1007/978-981-10-7575-9_12.